

## Filler Networks in Elastomers

*Françoise Ehrburger-Dolle,\*<sup>1</sup> Françoise Bley,<sup>2</sup> Erik Geissler,<sup>1</sup> Frédéric Livet,<sup>2</sup> Isabelle Morfin,<sup>1</sup> Cyrille Rochas<sup>1</sup>*

<sup>1</sup> Laboratoire de Spectrométrie Physique, UMR 5588 CNRS - Université Joseph Fourier de Grenoble, BP 87, F-38402 Saint Martin d'Hères Cedex, France

<sup>2</sup> Laboratoire de Thermodynamique et Physico-Chimie Métallurgiques, UMR 5614, INPG, F-38402 Saint Martin d'Hères Cedex, France  
E-mail: fehrburg@spectro.ujf-grenoble.fr

**Summary:** Elastomers are soft materials that can be reinforced by dispersing into them nanosized solid particles. Common examples of the latter are silica or carbon black aggregates. However, the mechanism of reinforcement is still not yet fully understood. Our work consists in investigating by small-angle X-ray scattering (SAXS) the structure of the aggregate network spreading throughout the matrix in the initial sample and its modification during and after straining (elongation). The goal is to relate the macroscopic mechanical behaviour with the structure of the aggregate network. The present paper is a qualitative overview of recent results obtained on well defined composites.

**Keywords:** cross-linking; elastomers; mechanical properties; reinforcement; SAXS

### Introduction

Modification of the mechanical properties (or reinforcement) of elastomers with colloidal particles is a well known fact that has been widely investigated but its mechanism still remains not fully understood. Recent progress has been made by examining the role of the long range structure of the filler network in theoretical approaches<sup>[1]</sup> and, in experiments, by means of small angle scattering measurements.<sup>[2–5]</sup> The complexity of the problem of reinforcement is due to the large number of parameters involved in the preparation of the sample. It is also due to the fact that fillers generally consist of mass fractal aggregates (*e.g.*, carbon black), whereas only spherical particles were considered in the first series of papers.<sup>[2–3]</sup> Therefore, we intended to investigate a series of well defined composites. The parameters involved are the type of elastomer (EPR and SBR), whether it is cross-linked (dicumyl peroxide) or not and the type of filler (carbon black, hydroxylated or hydrophobic pyrogenic silicas). SAXS and uniaxial stretching measurements are performed on samples originating from the same batch.

## Experimental

The elastomer matrices are ethylene-propylene rubber (EPR, Buna AP 301) or styrene butadiene rubber (SBR, Duradene 706). Commercial fillers investigated are carbon black N330 (Sid Richardson), fume hydroxylated (Aerosil 200, Degussa) and hydrophobized (Aerosil R974, Degussa) silica. The cross-linking agent is dicumyl peroxide. Dispersion, performed under the same standard conditions for all samples, is followed by calendaring (*ca.* 1 mm sheets). For all samples, the filler concentration is close to 40 phr, corresponding to a volume fraction  $\phi$  close to 0.20 and 0.17 for carbon black and silica respectively. To investigate the arrangement of aggregates,<sup>[4-5]</sup> SAXS measurements in the low  $q$  domain were performed on the BM2 beamline at the European Synchrotron Radiation Facility (ESRF, Grenoble, France). Two-dimensional scattering patterns were obtained with a CCD camera. Stress-strain curves were obtained with an extensometer (RHEO, TA XT2). For this series of experiments, owing to the particular shape of the probe, the exact value of the section of the sample may be underestimated and, hence, the absolute value of the stress may be overestimated. However, it is reasonable to assume that the relative values from one sample to another are correct.

## Results and Discussion

The first series of results concerns elastomers filled with carbon black (CB). For an uncross-linked EPR matrix (Figure 1), the scattering pattern is isotropic both for the initial unstrained sample and for small strains. For a value of the strain  $\epsilon=0.27$ , the pattern becomes anisotropic. For  $\epsilon=0.53$ , it displays a characteristic "butterfly" shape. In the latter case, the SAXS intensity curves measured along the direction parallel ( $I_{\parallel}$ ) and perpendicular ( $I_{\perp}$ ) to the stretch axis (Figure 2, right) are no longer identical, as they were for undeformed or weakly elongated samples (Figure 2, left). The physical meaning of such curves has been discussed in detail in previous papers.<sup>[4-5]</sup> In brief, the power law domain observed in a log-log plot of the scattered intensity  $I(q)$  results from the structure factor of CB fractal aggregates ( $D_f \cong 1.8$ ). The value of the slope is close to  $-1.8$  for dilute dispersions. The slightly lower absolute value (1.5) measured for the initial sample (Figure 2, left) indicates that CB aggregates form a connected network of slightly interpenetrating aggregates. For  $\epsilon=0.53$ , the aggregates strongly interpenetrate each other in the direction perpendicular to elongation (compaction). In the

direction of elongation,  $I(q)$  becomes similar to that measured for isolated CB aggregates. This observation suggests that CB aggregates become less interpenetrated along the stretch direction.

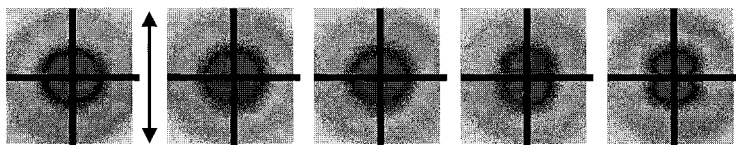


Fig. 1. Two-dimensional SAXS patterns from carbon black N330 dispersed in uncross-linked EPR. From left to right: the initial unstretched sample and samples stretched in the direction of the arrow at  $\epsilon=0.02$ ,  $\epsilon=0.07$ ,  $\epsilon=0.27$ ,  $\epsilon=0.53$ . The distance between the centre and any side of the square is equal to 50 pixels (corresponding to  $4 \times 10^{-2} \text{ nm}^{-1}$ ).

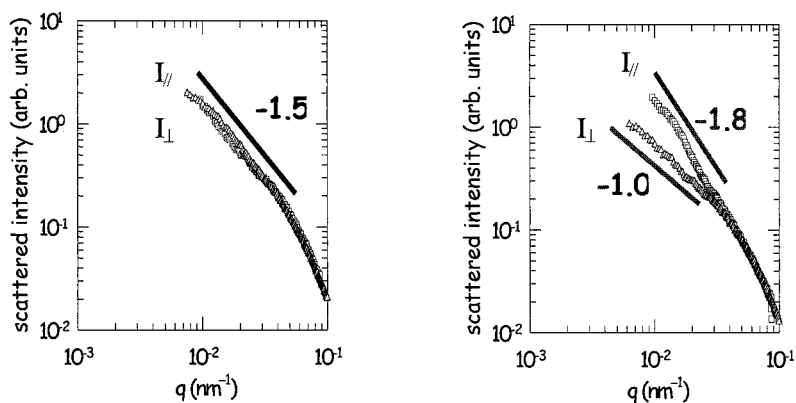


Fig. 2. SAXS intensity curves determined along the two directions (parallel and perpendicular to the direction of stretch) for the initial sample (left) and (right) for the stretched sample ( $\epsilon=0.53$ ).

The SAXS patterns measured for the cross-linked system (Figure 3) display no anisotropy in the same domain of  $q$  values. It was shown<sup>[3-4]</sup> that a similar feature is observed for concentrations below the percolation threshold, in uncross-linked EPR. Figure 4 (left) shows that cross-linking of the matrix induces strong interpenetration of the CB aggregates, thus

forming large agglomerates. Also, the mechanical behaviour of the two series of composites (Figure 4, right) is significantly different. The shape of the curve obtained for the uncross-linked system is characteristic of a hard material<sup>[2]</sup> in which the stiffness results from a network of slightly interpenetrating CB aggregates. It is worth noting that the appearance of the butterfly pattern that characterises the start of the disruption of the aggregate network coincides with the maximum of the stress-strain curve. Within the same range of strain, cross-linked systems are less stiff and do not display a maximum. Both SAXS and mechanical measurements on cross-linked EPR thus suggest that CB aggregates may be arranged into large agglomerates separated by a layer of polymer. Electrical conductivity measurements may be able to verify the above hypothesis.

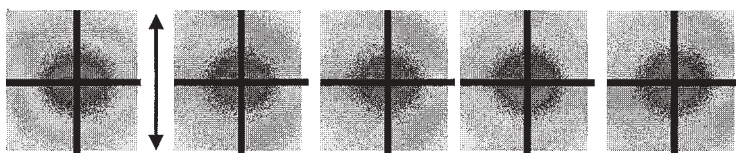


Fig. 3. SAXS patterns from carbon black N330 dispersed in cross-linked EPR. From left to right: before stretching, stretched at  $\epsilon=0.03$ ,  $\epsilon=0.07$ ,  $\epsilon=0.13$ ,  $\epsilon=0.27$ .

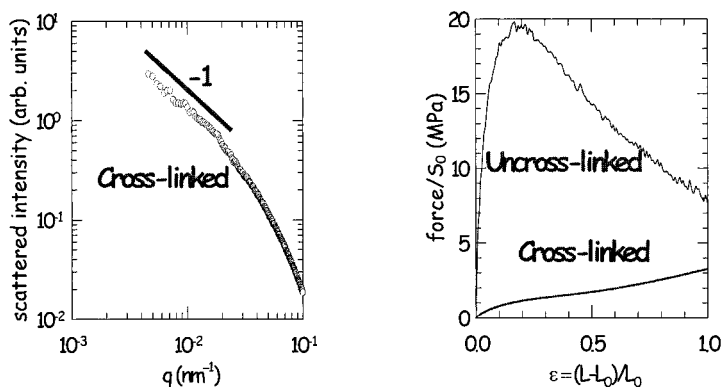


Fig. 4. (Left) Example of SAXS intensity curve for the cross-linked carbon black - EPR composite determined from any image shown in Figure 3. (Right) Comparison between the stress-strain curves measured for the uncross-linked and the cross-linked samples (*absolute values of the stress may be overestimated, see text*).

For the same amount of the same CB dispersed in SBR, the SAXS pattern is isotropic for the initial sample (and at small elongation), similarly to what is observed for dispersions in uncross-linked EPR, and a butterfly pattern is observed at larger strains. The SAXS intensity curve (Figure 6), however, indicates that CB aggregates in the initial sample are arranged into small strongly interpenetrated agglomerates (slope is equal to  $-1$  and  $I(q)$  displays an upturn at low  $q$ ).

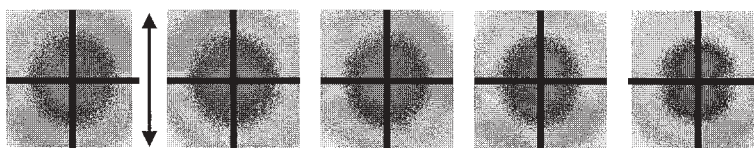


Fig. 5. Two-dimensional SAXS patterns from carbon black N330 dispersed in uncross-linked SBR. From left to right: before stretching, stretched at  $\varepsilon=0.03$ ,  $\varepsilon=0.07$ ,  $\varepsilon=0.12$ ,  $\varepsilon=0.25$ .

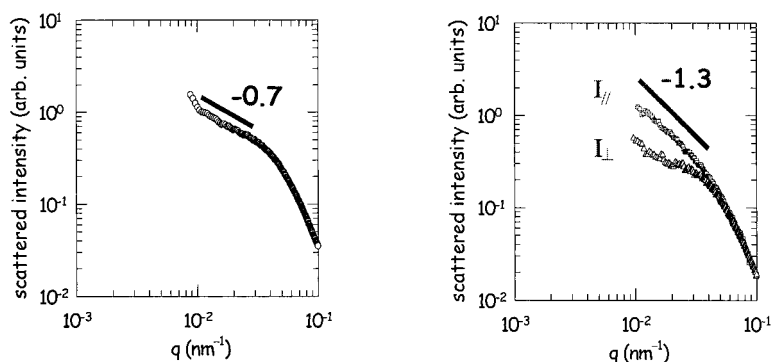


Fig. 6. SAXS intensity curves determined for uncross-linked carbon black - SBR composite, radially averaged for the initial sample (*left*) and (*right*) along the two directions for the stretched sample ( $\varepsilon=0.25$ ).

After cross-linking, the SAXS patterns also remain nearly isotropic (Figure 7). From the SAXS intensity curve (Figure 8, left), it can be deduced that the aggregates are now less mutually interpenetrating than in the uncross-linked sample. Moreover, the cross-linked sample is stiffer

than the uncross-linked one (Figure 6, right). More experimental work is necessary to go further into the analysis of the results obtained for SBR.



Fig. 7. Two-dimensional SAXS patterns from carbon black N330 dispersed in cross-linked SBR. From left to right: before stretching, stretched at  $\varepsilon=0.33$ ,  $\varepsilon=0.27$ ,  $\varepsilon=0.40$ ,  $\varepsilon=0.53$ .

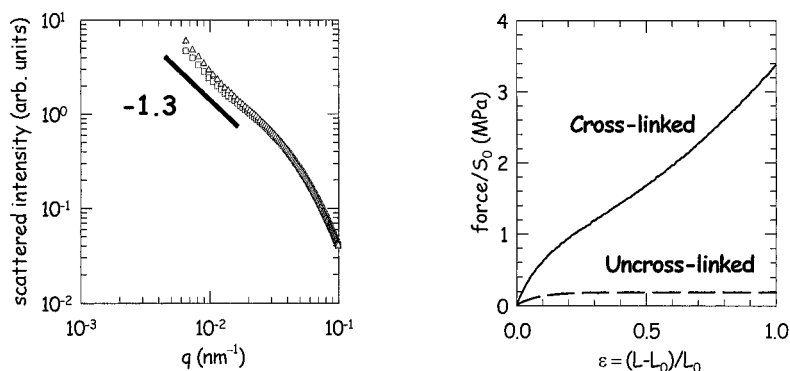


Fig. 8. (Left) Example of SAXS intensity curve for the crosslinked carbon black – SBR composite determined from any image shown in Figure 7. (Right) Comparison between the stress-strain curves measured for the uncross-linked and the cross-linked samples.

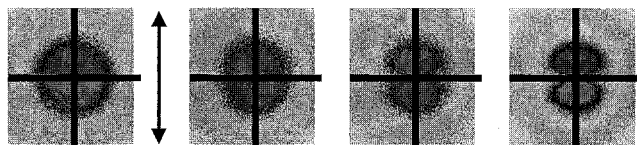


Fig. 9. Two-dimensional SAXS patterns from Aerosil 200 dispersed in uncross-linked EPR. From left to right: before stretching, stretched at  $\varepsilon=0.04$ ,  $\varepsilon=0.09$ ,  $\varepsilon=0.25$ .

For the second series of experiments the filler is hydroxylated (A200) or hydrophobic (R974) fume silica and the matrix is the same EPR as that used for CB. The SAXS patterns obtained

for A200 dispersed in uncross-linked EPR (Figure 9) show that appearance of anisotropy occurs at very small strain ( $\epsilon \leq 0.04$ ). For the initial sample, scattering is isotropic but the corresponding intensity curve (Figure 10, left) is very different from any curve measured for carbon black. It reveals the existence of fractal aggregates with  $D_f = 2.2$  and a radius of gyration  $R_g$  (determined by the Guinier equation) close to 53 nm. Such a result is expected if one recalls the well known characteristics of pyrogenic silicas. They consist of small primary aggregates (the "fume particles") that are able to build secondary aggregates. The number  $N$  of primary particles in primary aggregates is smaller than 10 and, for A200, their radius of gyration  $r_g$  is close to 5 nm. In air, a diffusion limited cluster-cluster aggregation (DLCA) process yields large secondary fractal aggregates with  $D_f$  close to 1.7. In a liquid, a gel is formed (the liquid does not flow owing to the silica aggregate network). As shown earlier,<sup>[6]</sup> the fractal dimension of the secondary aggregates depends on the relative interaction between the primary aggregates (solid-solid interactions such as H-bonds between surface hydroxyl groups) and between the silica surface and the dispersing medium. Figure 9 shows that, as for CB, scattering of the initial sample is isotropic. The corresponding SAXS intensity curve (Figure 10, left) is, however, very different. It indicates that A200 dispersed in EPR consists of fractal clusters (secondary

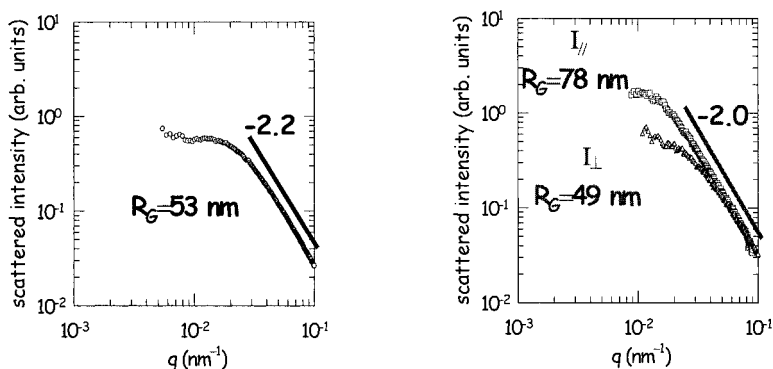


Fig. 10. SAXS intensity curves determined for uncross-linked Aerosil 200 - EPR composite, radially averaged for the initial sample (*left*) and (*right*) along the two directions for the stretched sample ( $\epsilon = 0.25$ ).

aggregates) that are more compact ( $D_f \approx 2.2$ ) than in air. The butterfly pattern appears at low strain ( $\epsilon \leq 0.04$ ). At larger strain ( $\epsilon = 0.25$ ), its shape (Figure 9) is different from that of the

strained CB composite (Figure 1). This difference is also revealed in the SAXS intensity curve (Figure 10, right): in the stretching direction, the secondary fractal aggregates become larger ( $R_g=78$  nm) but less compact. As a first approximation, the number  $N = (R_g/r_g)^{D_f}$  of primary particles remains constant ( $N \cong 200$ ).

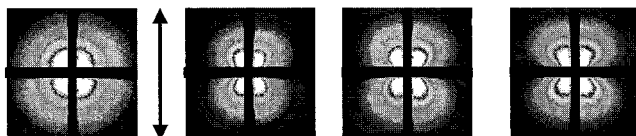


Fig. 11. Two-dimensional SAXS patterns from Aerosil 200 dispersed in cross-linked EPR. From left to right: before stretching, stretched at  $\varepsilon=0.12$ ,  $\varepsilon=0.25$ ,  $\varepsilon=0.52$ .

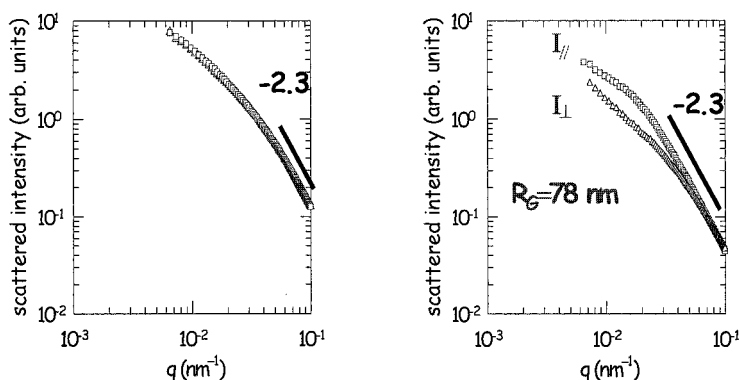


Fig. 12. SAXS intensity curves determined along the two directions for the initial sample (*left*) and (*right*) for the stretched sample ( $\varepsilon=0.52$ ).

Unlike CB, cross-linking of EPR containing A200 does not prevent anisotropy in strained samples (Figure 11), but it also induces a modification of the secondary aggregate structure in the initial sample (Figure 12). For the unstrained sample (Figure 12, left), the fractal domain is narrow and it is not possible to fit the low  $q$  data to a Guinier equation, *i.e.*, to determine a mean radius of gyration. For the strained composite ( $\varepsilon=0.52$ ), however, the SAXS intensity curve measured along the stretching direction (Figure 12, right) is similar to that obtained for the uncross-linked sample (Figure 10, right), but aggregates remain more compact ( $D_f \approx 2$  for



uncross-linked EPR). Comparison between the SAXS intensity curves measured before elongation (Figure 12, left) and parallel to the stretch (Figure 12, right) suggests that stretching breaks large secondary fractal aggregates into smaller ones (but still containing more than 500 primary particles).



Fig. 13. Two-dimensional SAXS patterns from Aerosil R974 (hydrophobic) dispersed in uncross-linked EPR. From left to right: before stretching, stretched at  $\varepsilon=0.03$ ,  $\varepsilon=0.11$ ,  $\varepsilon=0.17$ .

For hydrophobic A200 (or R974), the butterfly pattern (Figure 13) becomes visible at a larger strain than for hydroxylated A200. In other respects, the fractal dimension of the secondary aggregates is slightly smaller (Figure 14).

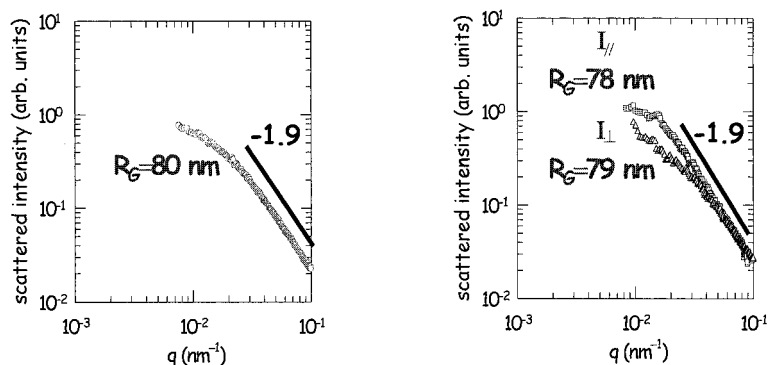


Fig. 14. SAXS intensity curves determined for uncross-linked Aerosil R974 - EPR composite, radially averaged for the initial sample (*left*) and (*right*) along the two directions for the stretched sample ( $\varepsilon=0.17$ ).

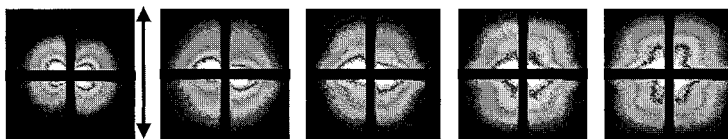


Fig. 15. Two-dimensional SAXS patterns from Aerosil R974 (hydrophobic) dispersed in cross-linked EPR. From left to right: before stretching, stretched at  $\varepsilon=0.27$ ,  $\varepsilon=0.40$ ,  $\varepsilon=0.53$ ,  $\varepsilon=0.67$ .

After cross-linking of the matrix the SAXS pattern from R974 (Figure 15) before elongation displays the butterfly shape that was observed for the previous samples after elongation. Thus, for this sample, calendaring induces frozen-in anisotropy. It is worth noting that a similar feature was already observed for carbon black dispersed in polyethylene.<sup>[4]</sup> By chance, elongation was directed perpendicularly to the initial anisotropy. Figure 15 shows, at least qualitatively, that the silica aggregates tend to rearrange at increasing strains, finally yielding a butterfly pattern oriented parallel to the stretch direction. It seems likely that not only the SAXS patterns but also the stress-strain curve (Figure 16, right) could be significantly different if the samples are cut from the sheet in a different direction.

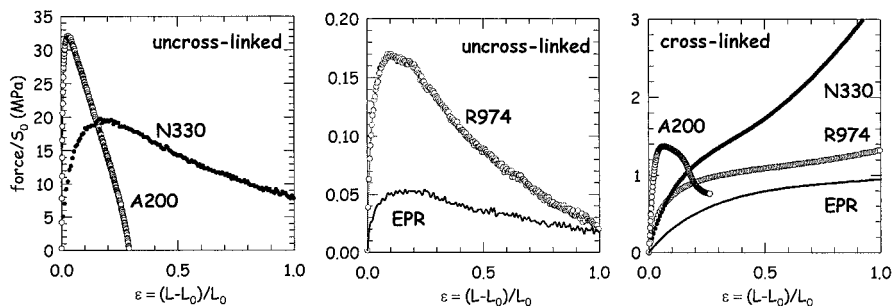


Fig. 16. Comparison of the stress-strain curves for the different EPR-filler composites.

The effect of cross-linking on the mechanical behaviour of unfilled EPR is shown in Figure 16 (centre and right). For uncross-linked, unfilled or filled EPR, the stress-strain curve exhibits a maximum that coincides with the appearance of the butterfly in the SAXS pattern. It follows that the decrease of the stiffness above a yield strain starts when the solid aggregate network begins to break. Such behaviour is similar to shear thinning in fluids gelled by silica.<sup>[17]</sup>

Interestingly enough, the network consisting of hydroxylated silica aggregates is far stiffer than without surface OH groups. This feature is fully consistent with the existence of H-bonds in the former. For carbon black, stress-strain curves measured for cross-linked EPR or SBR keep increasing up to the break point, as commonly reported in the literature.<sup>[1]</sup> Unlike carbon black, fume silica in cross-linked EPR always exhibits a maximum in the stress-strain curve where the butterfly pattern becomes visible. This feature suggests that, with silica, cross-linking does not hinder the formation of a network of secondary fractal aggregates, which gives stiffness but less extensibility. It also explains the need for surface treatment and/or inter-aggregate coupling agents when silica is used as a reinforcement filler.

## Conclusion

The experimental results obtained by SAXS for the series of samples reported above clearly show that the morphology of the secondary aggregates depends on several parameters as does the mechanical behaviour. Therefore, SAXS measurements are essential for investigating the validity and/or universality of theoretical models describing reinforcement.

## Acknowledgements

We express our gratitude to Michel Gerspacher, Leszek Nikiel (Sid Richardson, USA) and Guy Evrard (LRCCP, France) for their help in the preparation of the samples and to Jean-Patrick Bazile and Vivien Aromatario (LSP, Grenoble) for mechanical measurements. We are also grateful to the ESRF for access to the beamline BM2 and to the French CRG team (Jean-François Béar, Bernard Caillot, Nathalie Boudet and Stephan Arnaud).

[1] G. Heinrich, M. Klüppel, *Adv. Polym. Sci.* **2002**, *160*, 1; M. Klüppel, *this issue*.

[2] Y. Rharbi, B. Cabane, A. Vacher, M. Joanicot, F. Boué, *Europhys. Lett.* **1999**, *46*, 472.

[3] S. Westermann, M. Kreitschmann, W. Pyckhout-Hintzen, D. Richter, E. Straube, B. Farago, G. Goerigk, *Macromolecules* **1999**, *32*, 5793.

[4] F. Ehrburger-Dolle, M. Hindermann-Bischoff, E. Geissler, C. Rochas, F. Bley, F. Livet, *Langmuir* **2001**, *17*, 329.

[5] F. Ehrburger-Dolle, M. Hindermann-Bischoff, E. Geissler, C. Rochas, F. Bley, F. Livet, *Mater. Res. Soc. Symp.* **2001**, *661*, KK7.4.1.

[6] F. Ehrburger, R. Jullien, in: "Characterization of Porous Solids I", K.K. Unger, J. Rouquérol, K.S.W. Sing, H. Kral, Eds., Studies of Surface Science and Catalysis vol. 39, Elsevier, Amsterdam 1988, pp. 441-449.

[7] E. Geissler, A.-M. Hecht, C. Rochas, F. Bley, F. Livet, M. Sutton, *Phys. Rev. E* **2000**, *62*, 8308.

